SI Appendix.

SI Materials and Methods

Plant materials and growth conditions. *Arabidopsis thaliana* Columbia (Col-0) wild-type and *cpl2-2* (SALK_059753) were obtained from The Arabidopsis Information Resource. For cotyledon cell shape analysis, seeds were cold-treated at 4 °C for 4 days and then grown on soil for 7 days at 24°C with 16 hr light/8 hr dark cycle. For RPB1 protein phosphorylation analysis, seeds were surface sterilized and cold-treated at 4 °C for 4 days and cultured in 50 ml half strength Murashige and Skoog (MS) basal salt media supplemented with 1% sucrose, shaking at 150 rpm for 5-6 days at 22°C with 12 hr light/12 hr dark cycle. Under the same growth condition, 6-day-old seedlings were used for CPL1-FAST degradation analysis, and 4-day-old seedlings were treated with 1μm NAA for 4 hrs and then harvested for measuring CTD phosphorylation. For RT-PCR analysis, seeds were surface sterilized and cold-treated at 4 °C for 4 days and grown on Phytoblend-solidified half strength MS medium supplemented with 1% sucrose for 7 days at 25°C. For transgenic plants first described in this paper, homozygous plants of T3 or T4 generations were used in most of phenotypic characterization and biochemical or gene expression studies. At least four independent homozygous lines were used for initial Western blot and phenotypic studies and one of these that showed similar results to other lines was chosen as a representative for presentation in all figures.

Map-based cloning and complementation test. Map-based cloning was preformed according to (1). *cae2-1* CA1-1 was crossed to ecotype Landsberg *erecta* and 463 F2 seedlings with *cae2-1* CA1-1 phenotype were selected. Sequence length polymorphism (SSLP) markers were used for rough mapping and *CAE2* was first located around marker ciw7, between F17L22M1 and T8O5M1, on chromosome 4. Fine mapping eventually mapped the *CAE2* gene to a region of 186 Kb. Subsequently, open reading frames for a total of 52 candidate genes located in this region were amplified and sequenced to determine the mutation. To complement the *cae2-1*CA1-1 phenotype, an expression cassette including a 7.7 kb *CPL1* genomic fragment, containing 1.6 kb 5' upstream of ATG, 5.4 kb ORF and 0.7 kb 3' downstream of the stop codon TAA, was constructed by ligating two smaller fragments, which were PCR-amplified using primer pairs CZP194/CZP195 and CZP201/CZP196 and subsequently sequence verified, into the transformation vector pCAMBIA1301. Primers CAM2 and CZP104 were used to identify transgenic plants, and CZP278 and CZP262 were used to examine the wild type *CPL1* transcript. Primers are listed in Supplementary Table S1.

RNA sequencing data analysis. Shoots were harvested from seven-day-old seedlings of WT, CA1-1, *cae2-1*, *cae2-1* CA1-1 grown vertically on agar-solidified ½ MS medium with 1% sucrose and RNA was extracted. Each genotype had two biological replicates. Total RNA samples were sent to Beijing Genomics Institute (BGI) Tech Solutions Co. in Shenzhen, China, for library construction, sequencing, data preprocessing and gene mapping. Briefly, total RNA was treated with DNase I and mRNA was enriched through the oligo(dT) magnetic beads. Following fragmentation, short mRNA fragments were used for cDNA synthesis, and the purified the double stranded cDNA is used for construction of the sequencing library. Sequencing was performed via Illumina HiSeqTM 2000. Raw data were preprocessed by removing adaptor sequences and/or low quality reads, resulting in clean reads data. These clean

reads data were then mapped to the Arabidopsis reference genome using SOAP aligner/SOAP2 (2). Differentially expressed genes between two genotypes were identified using the exact test for negative binomial models implemented in EdgeR (3). The common dispersion, tagwise dispersion, and the exact test were estimated by or based on the quantile-adjusted conditional maximum likelihood (qCML) method. The qCML method is regarded as the most reliable method and specifically suitable for experiments with very small sample size. Statistically significant genes had at least 2-fold changes and a FDR value less than 0.1. Hierarchical clustering analysis was performed to identify genes with similar expression patterns. Specifically, the complete linkage clustering with Pearson correlation-based cluster distance measure was used. Cell wall-related genes were identified by Gene Ontology (GO) enrichment analysis using the hypergeometric test provided in AgriGO (4), with the Yekutieli-based adjustment for multiple testing (FDR under dependency; a cutoff of FDR at 0.05).

Plasmid construction. For UBCA1 overexpression vector, a 1.0 kb *UBQ10* promoter fragment was PCR-amplified using primers ZZP6 and ZZP7 and cloned into a previously constructed vector ZZ103, which contains 1.3 kb *ROP2* promoter:CA-rop2, resulting in ZZ105 which replaced *ROP2* promoter with the *UBQ10* promoter. Subsequently, the BamHI-BstEII (fill-in) digested fragment of *UBQ10:CA-rop2* was ligated with the BamHI and SstI (fill-in)-digest pBI101 vector, resulting in GZ47, which converted Hyg^R into Kan^R in the expression vector.

For 35S:*CPL1* overexpression vector, the full-length *CPL1* coding sequence was cloned by ligating two fragments, *CPL1-N* (1-1615 bp) and *CPL1-C* (922-2904 bp). CPL1-N was amplified from cDNA using primers CZP192 and CZP195 and inserted into GZ0 vector using BglII/NcoI sites. Subsequently, *CPL1-C* (922-2904bp), amplified using primers CZP181 and CZP193, was inserted into the NcoI/XbaI (fill-in) sites of the vector containing *CPL1-N*, resulting in the vector CZ17. After sequencing verification, the full-length *CPL1* coding sequence was PCR-amplified from CZ17 using primers BZP20 and BZP21 and inserted into the pFGC5941 vector using XhoI/BamHI sites, resulting in the vector BZ01.

For *35S:CPL1-FAST* construct, FAST (Flag And Strep II Tags) sequence was amplified from pBI-FAST with primers ZZP10 and BZP133 and inserted into ZL02 vector using BamHI/PmlI sites, resulting in ZL02-FAST. *CPL1* coding sequence was amplified from CZ17 using primers BZP134 and BZP132 and inserted into ZL02-FAST vector using PstI/BamHI sites, resulting in BZ02.

For the fission yeast inducible *CA-rop2* expression vector, the coding sequence of Arabidopsis *CA-rop2* was amplified from plasmid ZZ105 using primers BZP81 and BZP82 and cloned into yeast vector pREP at the BamHI/NotI sites (NotI site fill-in) driven by the *nmt1* promoter, resulting in BZ04.

For the budding yeast inducible CA-rop2 expression vector, the *CA-rop2* coding sequence was amplified from plasmid ZZ105 using primers BZP81 and BZP82 and cloned into the yeast vector DZ37 (5) at the BamHI/XbaI sites driven by the *GAL1* promoter, resulting in BZ06.

Regular and quantitative RT-PCR. Total RNA was extracted from 7-day-old seedlings. For regular RT-PCR analysis of *CAE2* transcript (Figure 1D), primers CZP17 and CZP18 (Table S1)

were used. For quantitative real-time PCR analysis of *ROP2*, *CA-rop2*, *PME17*, *WAK1* and At2g47550/invertase genes, the gene-specific primers, BZP78 and BZP79 (for endogenous *ROP2*), BZP78 and BZP187 (for *CA-rop2*), BZP78 and BZP80 (for *CA-rop2* in UBCA background), BZP106 and BZP107 (for *PME17*), BZP100 and BZP101 (*WAK1*) and BZP145 and BZP146 (At1g47550), were designed (Table S1) and SYBR®Green dye was used in Master Cycler. PCR results were normalized to *ACT2*. Values were expressed as means of three replicates with standard deviation (SD).

For quantitative real-time PCR analysis in yeast, total RNA were isolated from overnight culture. Cells were resuspended in 1 ml TRIzol Reagent (Life technologies) and lysed by vortexing with 0.2 ml glass beads (Sigma, G8772). After chloroform extraction, isopropanol precipitation and 75% ethanol wash, RNA pellet was resuspended in water and treated with DNase. Five micrograms of total RNA were used for reverse transcription. Gene specific primers BZP193 and BZP194 (for *Rho1*), BZP213 and BZP214 (for *Rga1*) and BZP205 and BZP206 (for *Pmc5*) were designed (Table S1). Gene expression levels were normalized to the 28S rRNA internal control. Values were expressed as means of three replicates with standard deviation (SD).

Western blot. For plant protein experiments, seedlings were ground in liquid nitrogen into fine powder and extracted with the extraction buffer (25 mM Hepes pH7.4, 10 mM MgCl2, 100 mM NaCl, 5 mM DTT, 5 mM NaF, 1 mM PMSF, protease inhibitor cocktail (Sigma, Cat. P9599) and 1% Triton X-100). After 1 min vortex and centrifuge, protein samples were mixed with 10X SDS loading buffer and boiled for 10 min. For yeast protein experiments, cells were collected and resuspended in the SDS loading buffer and mechanically disrupted by vortexing with glass beads (Sigma, G8772). For extracting proteins from the budding yeast nuclear fraction, a yeast nuclei isolation kit was used (BioVision, K289-50) following manufacturer's instructions. After centrifuge, protein samples were boiled for 10 min. Samples were then separated by SDS-PAGE and transferred onto a PVDF membrane. The following antibodies were used in this study for immunoblots: anti-Ser5p (Abcam; ab5131), anti-Ser2p (Abcam; ab5095), both of which have been used to specifically detect Arabidopsis Ser2- or Ser5-phosphorylated CTD (6), anti-Ser7p (Active Motif, Clone 4E12), Arabidopsis Pol II Antibody (at-300) (Santa Cruz; sc-33754), ROP2 antibody (Sigma; R9529), anti-CTD (Abcam; ab26721), anti-FLAG (Sigma; F3165), anti-α-tubulin (Sigma; T6074), stabilized Goat anti-Mouse HRP-Conjugated (Pierce, 1858413), stabilized Goat anti-Rabbit HRP-Conjugated (Pierce, 1858415), and Goat anti-Rat HRP-Conjugated (Thermo, 31470). To detect CPL1-FAST, the fusion protein was purified with anti-Flag-conjugated beads (Sigma, A2220) from crude extracts and then detected by anti-FLAG antibody. For Fcp1 detection in budding yeast, a polyclonal anti-Fcp1 antibody (7) was used, and a Flag antibody (Sigma; F3165) was also used to detect the 3 x Flag-tagged Fcp1 (Fcp1-3xFlag). After antibody incubation, membrane was incubated with the chemilluminescent substrate (Thermo, 34096) following manufacturer's recommendations. Signal intensity was acquired by exposure to X-ray film.

CPL1 and Fcp1 protein degradation. For *in vitro* CPL1 protein degradation, CPL1-FAST protein was purified using anti-Flag antibody-conjugated beads from transgenic plants and mixed with equal amount of total protein crude extracts of WT and CA1-1, respectively, in the presence of 1 mM ATP. After incubation for 0, 45 min and 90 min at room temperature, with or without protein degradation inhibitors MG132 (50 μm) and lactacystin (20 μm), proteins were detected

using Western blot with an anti-Flag antibody. For *in vivo* Fcp1 protein degradation, nuclear extracts from the budding yeast transformants carrying CA-rop2 expression vector were detected using an anti-Fcp1 antibody (7) or an anti-Flag antibody for the 3xFlag-tagged Fcp1 strain with or without protein degradation inhibitors MG132 (50um) and lactacystin (20um).

Cotyledon cell imaging and quantitative analysis. Seedlings were grown on soil for 3-7 days and used for cotyledon cell shape observation. Cell imprinting was performed with 3% agarose as described (8). To observe pavement cell directly, cotyledons were collected and soaked in water/ethanol/acetic acid (1:3:3) for 4-8 hrs as described elsewhere (9). After treatment with 7% NaOH (dissolved in 61% ethanol) for 15min, 40% ethanol for 20min, 20% ethanol for 20min and 10% ethanol for 20min, cotyledon cells are ready for observation. Area and perimeter were measured using ImageJ. The shape factor was determined using the formula ($4\pi\times$area/perimeter^2) as described (10) after measuring the areas and perimeters for 60 cells (15 cells for each seedling cotyledon) for each genotype. Cell number was estimated by dividing the cotyledon area by the average cell area. Statistical analysis was performed using one-way or two-way ANOVA and Spearman correlation.

Yeast growth and transformation. The wild-type *Schizosaccharomyces pombe* strain (*h- ade6-M210 leu1-32 ura4-D18*) and mutant strain *cdc42-1625* (*h+ cdc42-1625(A158V)-kanMX leu1-32 ura4-D18*), *S. pombe* S2A, $(S5)_3(S5A)_{11}$ and $(S5)_2(S5A)_{12}$ mutant strains and their wild-type (*leu1-32, ura4-D18, his3–D1, ade6*), *Saccharomyces cerevisiae* wild-type strain W303-1B (5) and the Fcp1-3xFlag strain were used in this study. Yeast stains were cultured in YPAD medium (for *cdc42-1625* and its WT strain), EMM medium (for fission yeast transformants) or SC minimal medium (for budding yeast transformants). Electroporation method was used for yeast transformation. Transformants were selected by Leu-deficient EMM or SC medium supplemented with adenine, thiamine and uracil and further verified by extracting genomic DNA and PCR amplification with primers BZP81 and BZP82. Protein expression in fission yeast was induced when cells were cultured without thiamine for fission yeast or in the presence of galactose for budding yeast.

References

1. Lukowitz W, Gillmor CS, & Scheible WR (2000) Positional cloning in Arabidopsis. Why it feels good to have a genome initiative working for you. *Plant physiology* 123(3):795-805.
2. Li R*, et al.* (2009) SOAP2: an improved ultrafast tool for short read alignment. *Bioinformatics* 25(15):1966-1967.
3. Robinson MD, McCarthy DJ, & Smyth GK (2010) edgeR: a Bioconductor package for differential expression analysis of digital gene expression data. *Bioinformatics* 26(1):139-140.
4. Du Z, Zhou X, Ling Y, Zhang Z, & Su Z (2010) agriGO: a GO analysis toolkit for the agricultural community. *Nucleic acids research* 38(Web Server issue):W64-70.
5. Zhang B*, et al.* (2014) Aberrant gene expression in the Arabidopsis SULTR1;2 mutants suggests a possible regulatory role for this sulfate transporter in response to sulfur nutrient status. *The Plant journal : for cell and molecular biology* 77(2):185-197.

6. Ding Y, Avramova Z, & Fromm M (2011) Two distinct roles of ARABIDOPSIS HOMOLOG OF TRITHORAX1 (ATX1) at promoters and within transcribed regions of ATX1-regulated genes. *The Plant cell* 23(1):350-363.
7. Kobor MS*, et al.* (1999) An unusual eukaryotic protein phosphatase required for transcription by RNA polymerase II and CTD dephosphorylation in S. cerevisiae. *Molecular cell* 4(1):55-62.
8. Mathur J & Koncz C (1997) Method for preparation of epidermal imprints using agarose. *BioTechniques* 22(2):280-282.
9. Yang K*, et al.* (2014) Requirement for A-type cyclin-dependent kinase and cyclins for the terminal division in the stomatal lineage of Arabidopsis. *Journal of experimental botany* 65(9):2449-2461.
10. Kirik V*, et al.* (2007) CLASP localizes in two discrete patterns on cortical microtubules and is required for cell morphogenesis and cell division in Arabidopsis. *Journal of cell science* 120(Pt 24):4416-4425.

SI Figures

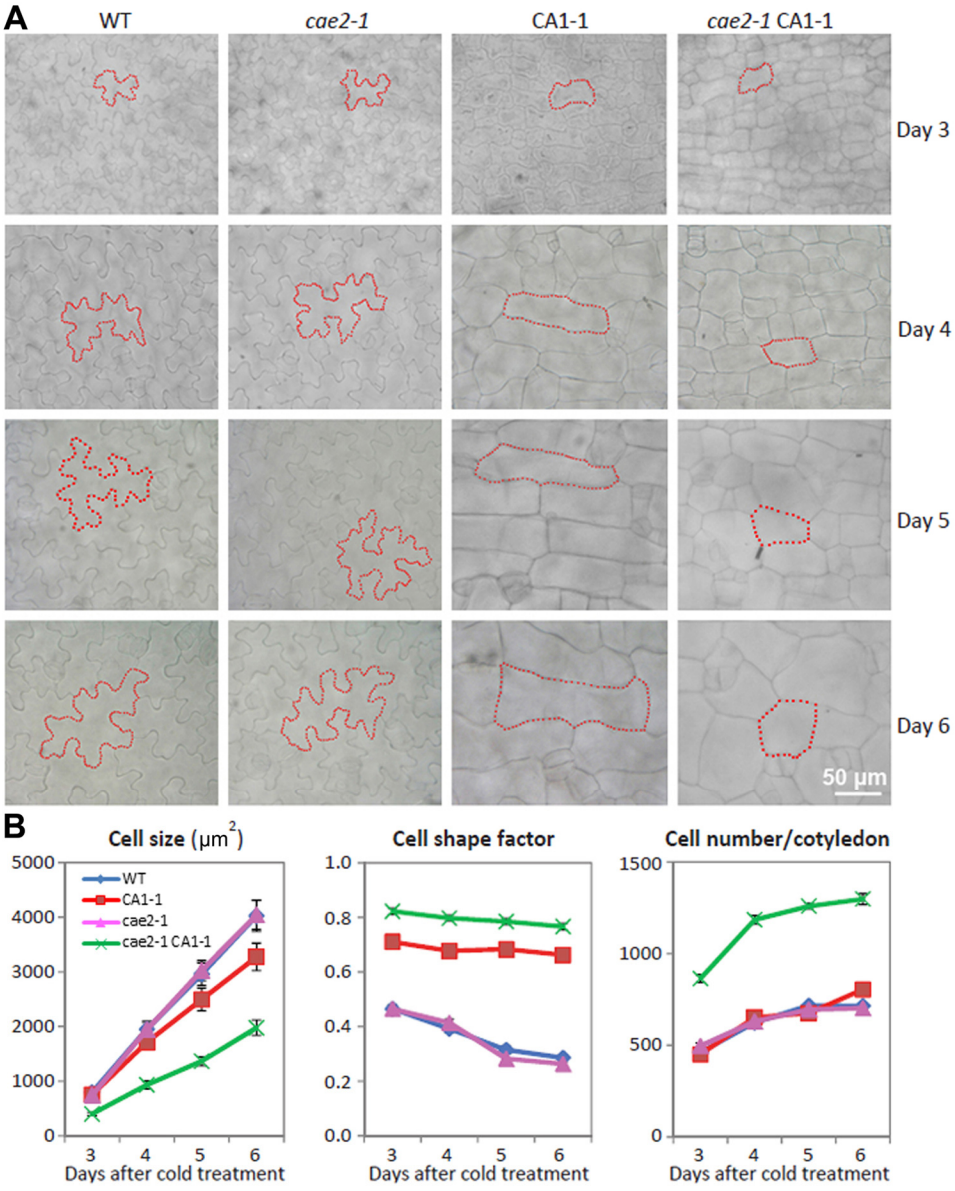

Fig. S1. Characterization of *cae2-1* CA1-1 cell growth and geometry parameters at various stages of pavement cell development.
(*A*) Representative cell images at various stages (Days 3-6 after cold-treatment of seeds) of cotyledon growth. WT, wild-type. (*B*) Quantitative analysis of pavement cell size, cell shape factor and cell number for each organ (cotyledon). Bar represents SEM of 60 cells (for size and shape) or 20 cotyledons (for cell number). Two-way ANOVA result shows that cell sizes for *cae2-1* and WT are not significantly different, while CA1-1 has a statistically significant difference (p-value <0.05) in cell size compared to WT only at Day 6, and *cae2-1* CA1-1 cell size is statistically different than WT and CA1-1 at all stages. For cell shape factor, *cae2-1* and WT are not significantly different, CA1-1 is statistically significant from WT at all stages, and *cae2-1* CA1-1 has a significant difference than both WT and CA1-1. Thus, *cae2-1* enhanced the

CA1-1 phenotypes of cell size and cell shape. For cell number, both *cae2-1* and CA1-1 are not statistically significant from WT, while *cae2-1* CA1-1 has a significant difference than all three other genotypes (WT, *cae2-1* and CA1-1). In addition, Spearman correlation analysis shows that *cae2-1* and WT have similarly strong negative correlations between cell size and cell shape factor (correlation coefficients of -0.88 for both genotypes), but the correlation in CA1-1 is weak (-0.49) and even weaker in *cae2-1* CA1-1 (-0.28). Furthermore, when controlling for the cell size effect, *cae2-1* CA1-1 still shows a statistically significant difference (p-value <0.001) in cell shape factor compared to WT. These results indicate that although *cae2-1* CA1-1 affects cell size and cell shape, this genotypic effect on cell shape cannot completely explained by the difference in cell size. In other words, the *cae2-1* mutation likely affects a process commonly involved in cell size and cell shape control and also a process controlling cell shape unrelated to cell size.

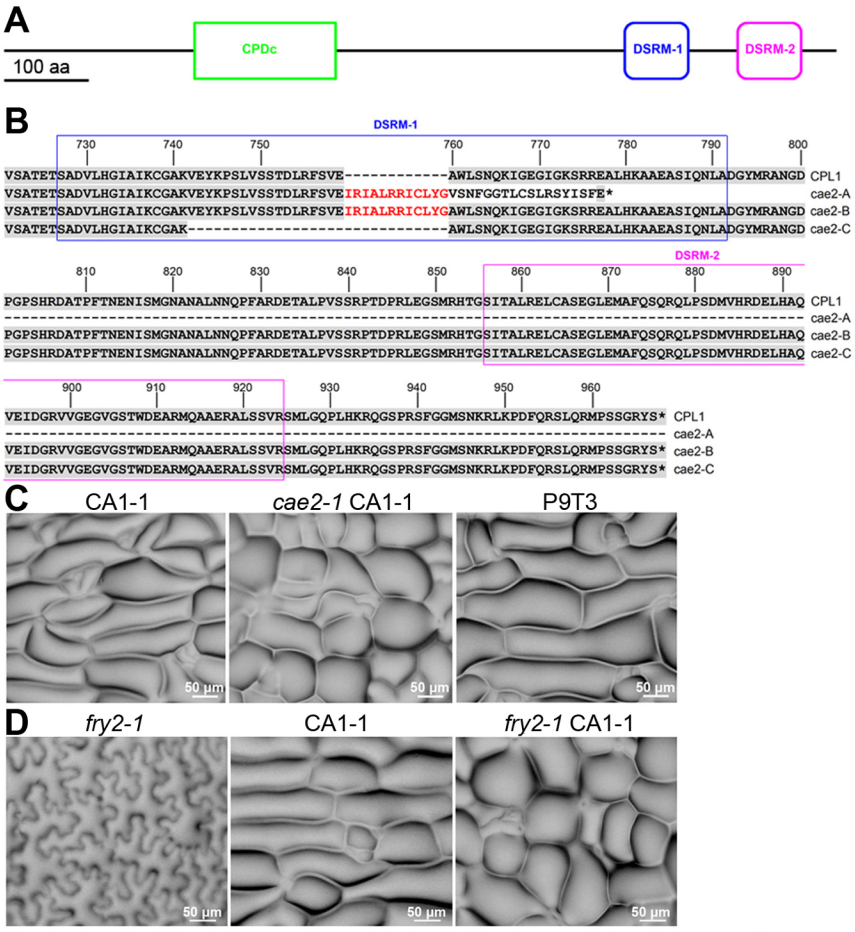

Fig. S2. Consequence of the *cae2* mutation on CPL1 protein amino acid sequence composition and allelic complementation of *cae2-1* by *fry2-1*.
(*A*) A schematic representation of CPL1 domain structure. CPDc, catalytic domain of ctd-like phosphatases; DSRM, Double-Stranded RNA Binding Motif. (*B*) Alignment of the predicted amino acid sequences derived from the three splicing variants in *cae2-1* (cae2-A, cae2-B and cae2-C) as shown in Fig.1D. Wild-type CPL1 protein sequence was included for comparison. The three forms of *cae2* splicing products altered the DSRM1 which was indicated by the blue box. Compared to CPL1, cae2-A contained amino acid residues that are truncated in DSRM1, cae2-B had an additional 12 amino acids inserted between 759 and 760 position of CPL1 protein, and cae2-C had 18 amino acids deleted at 742 and 759 positions. In summary, all of three alternatively spliced forms of *CAE2* mRNA in *cae2-1* are distinct from the full-length wild-type *CPL1* sequence, and if they were translated, they would encode the proteins with different mutations (deletion or addition) in DSRM1. It has been shown that both DSRM1 and DSRM2 are required for the proper function of CPL1, and thus we concluded that *cae2-1* represents a loss-of-function mutation of CPL1. (*C*) Functional complementation of *cae2-1* CA1-1 by transformation of a *CPL1* genomic fragment. A construct with a 7.7 kb *CPL1* genomic fragment, containing 1.6 kb upstream of ATG, 5.4 kb ORF and 0.7 kb downstream of stop codon, was transformed into *cae2-1* CA1-1. A representative transgenic line P9T3 exhibited the CA1-1-like cotyledon pavement cell shapes. (*D*) *cae2-1* is allelic to *fry2-1*. The *fry2-1* CA1-1 cotyledons had a similarly enhanced pavement cell shape defect as *cae2-1 CA1-1*.

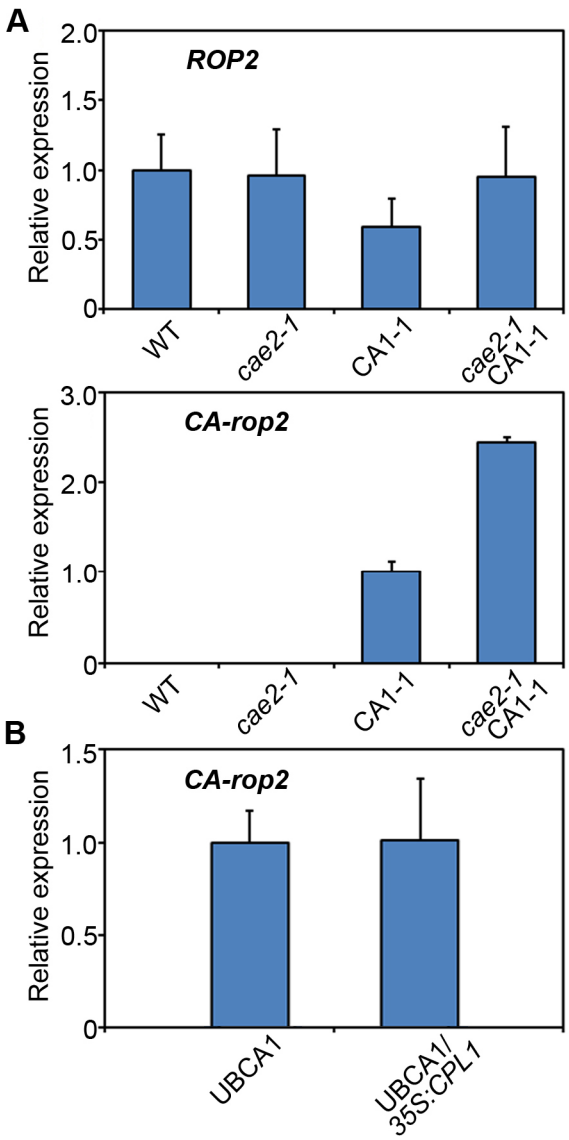

Fig. S3. qPCR analysis of *CA-rop2* transgene and endogenous *ROP2* gene expression. (*A*) Wild-type (WT), *cae2-1*, CA1-1, and *cae2-1* CA1-1. *Upper panel*, expression of endogenous *ROP2* gene. *Lower panel*, expression of transgenic *CA-rop2*. Transcript levels were normalized to that of *ACT2* internal control. The bar represents the SD for three biological replicates. (*B*) Similar expression of *CA-rop2* in UBCA1 and a transgenic line overexpressing *CPL1* in the UBCA1 background (UBCA1/*35S:CPL1*).

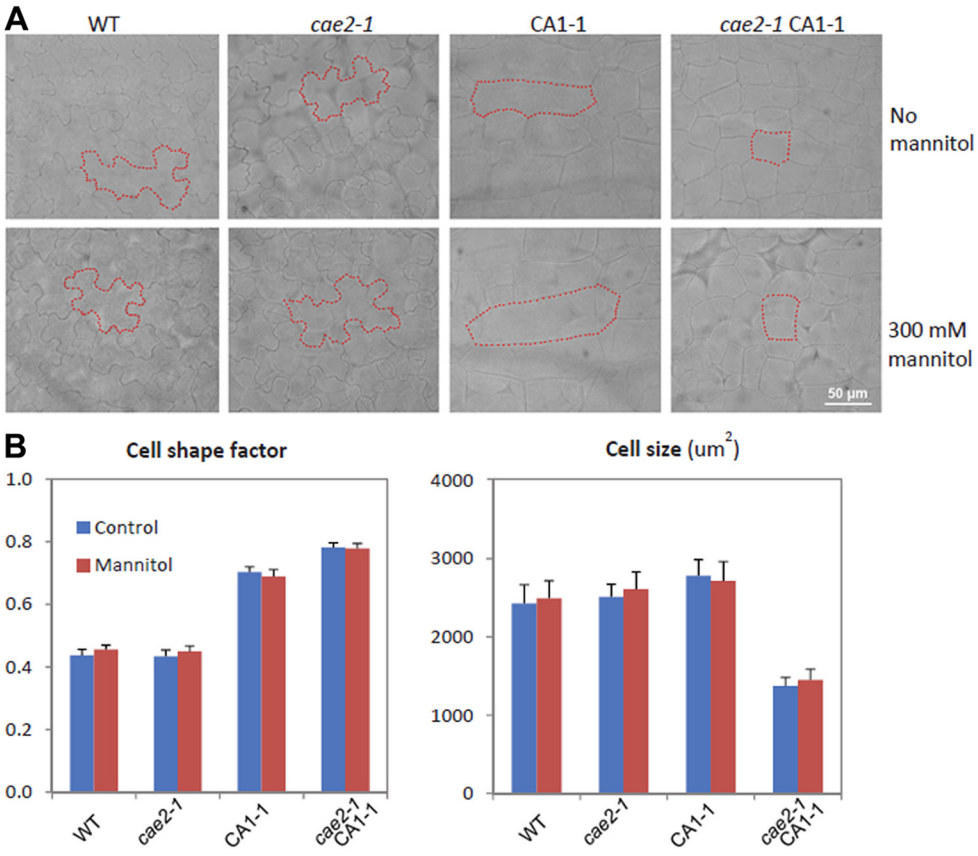

Fig. S4. Mannitol treatment does not phenocopy the effect of *cae2* mutation in enhancing the CA1-1 cell shape defect.
Upper panels, representative images showing cells after the osmotic treatment. 2-day-old young seedlings grown under normal medium (without mannitol) were treated with 0 or 300 mM mannitol for 3 days in liquid culture with 150 rpm shaking. *Lower panels*, quantitative analysis of pavement cell size and shape factor. Bar represents SEM of 40 cells. Two-way ANOVA result shows that the difference in cell size and shape factor between control and mannitol treatment in all genotypes is not significant, and thus the CA1-1 and the enhancer (*cae2-1* CA1-1) cell size and shape phenotypes were not due to the osmotic effect, as the mannitol treatment did not phenocopy the *cae2-1* mutation in the CA1-1 background. WT, wild-type.

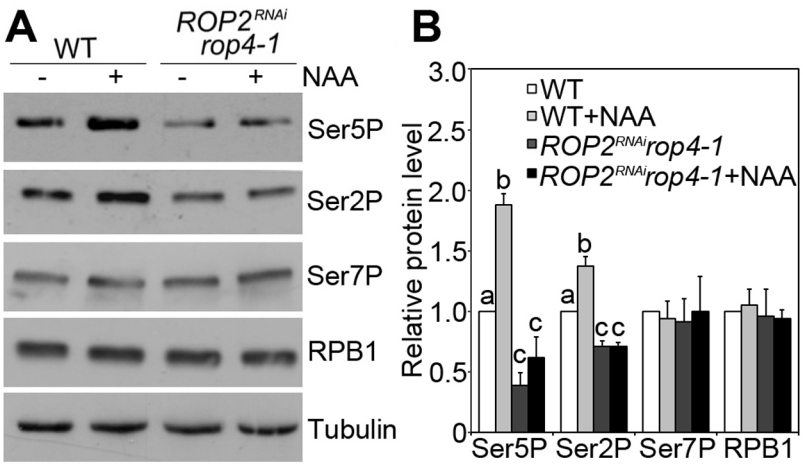

Fig. S5. Auxin-stimulation of CTD Ser5P and Ser2P is dependent on ROP2 and ROP4 activity. (*A*) Western blot images of Ser5P and Ser2P detection in wild-type (WT) and *ROP2*^{RNAi} *rop4-1* treated with or without 1 μM NAA for 4 hrs. (*B*) Quantitative analysis of Ser5P and Ser2P levels. Values are means ± SD (n=3 biological replicates), with different letters within the same category indicating a statistical difference (P<0.05; Pair-wise *t*-test).

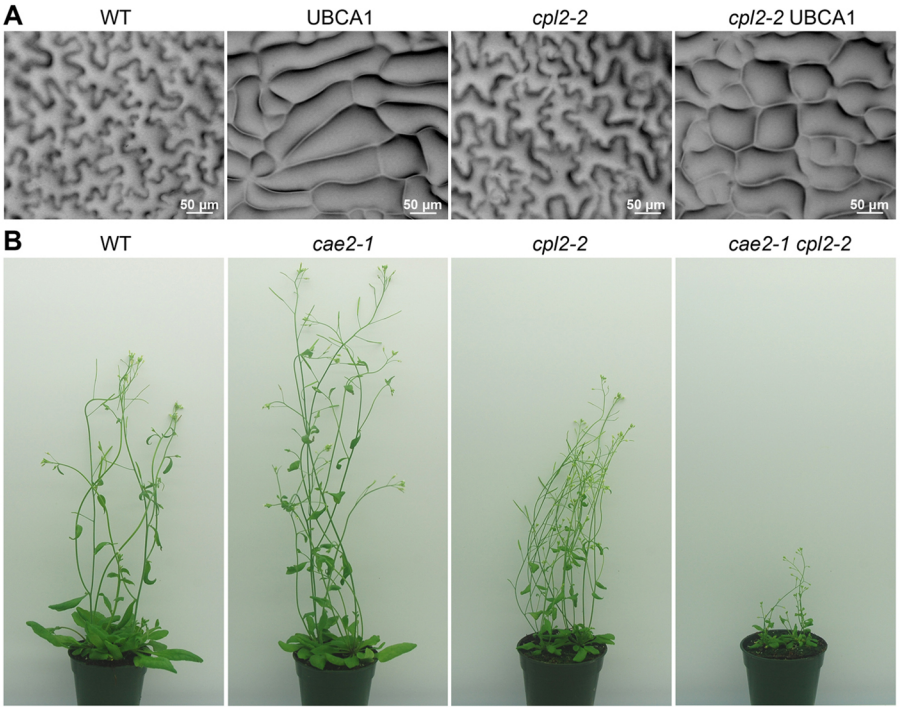

Fig. S6. CPL1 and CPL2 have redundant functions in cell shape, size and number and overall growth and development.
(*A*) *cpl2-2* enhanced the UBCA1 (*UBQ10:CA-rop2*) phenotype in cotyledon pavement cell shape, although itself did not show any pavement cell shape phenotype. WT, wild-type. (*B*) The *cae2-2 cpl2-2* double mutant exhibited severe growth reduction and were almost sterile.

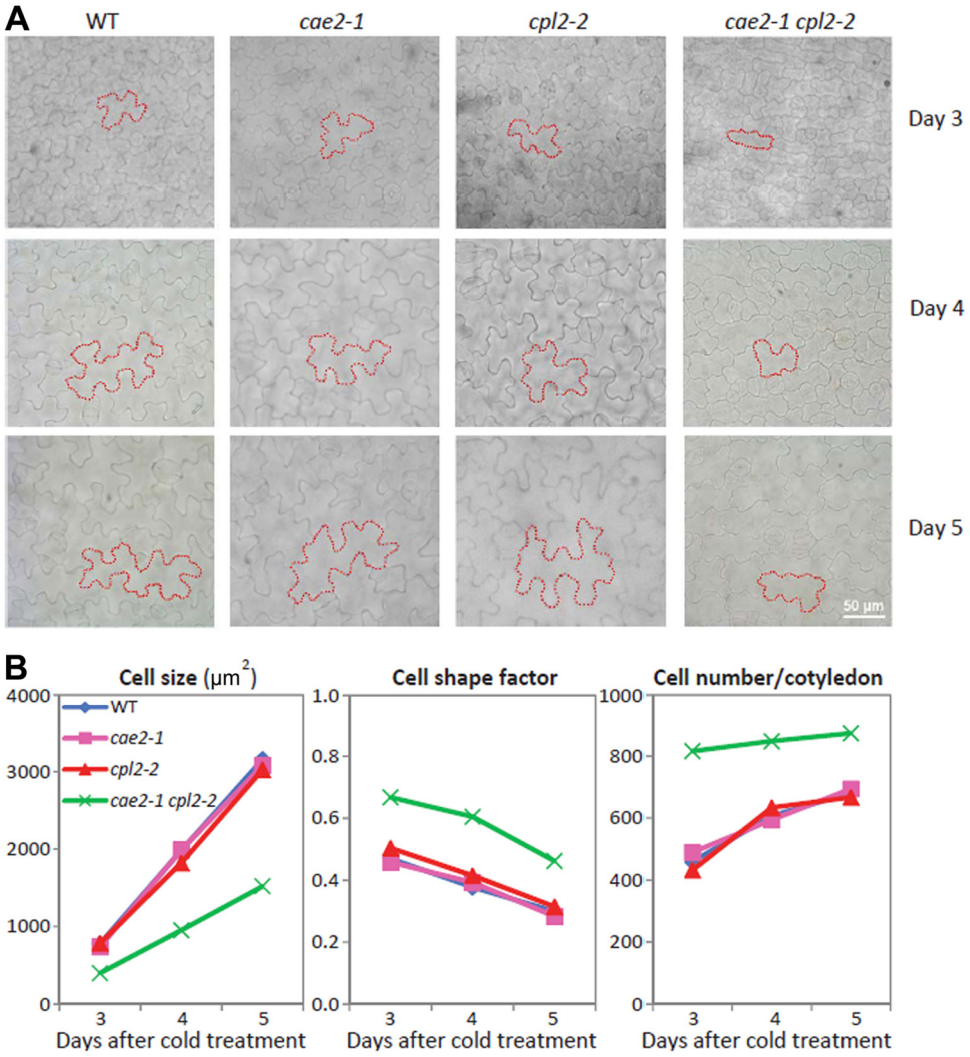

Fig. S7. The *cae2-2 cpl2-2* double mutant affected cotyledon pavement cell number, cell size and shape.
Upper panels, representative cell images at various stages (Days 3-5 after cold treatment of seeds) of cell shape formation. WT, wild-type. *Lower panels*, quantitative analysis of pavement cell size, shape factor and cell number for each organ (cotyledon). Bar represents SEM of 60 cells (for cell size and cell shape factor) or 20 cotyledons (for cell number). Two-way ANOVA result shows that *cae2-1 cpl2-2* has a statistically significant difference (p-value <0.05) in cell size, shape factor and cell number than all three other genotypes at all stages. Note that the smaller cell size in *cae2-1 cpl2-2* is unlikely due to developmental delay as after almost two weeks of growth, the double mutant still has smaller cells and true leaves have already developed similar WT.

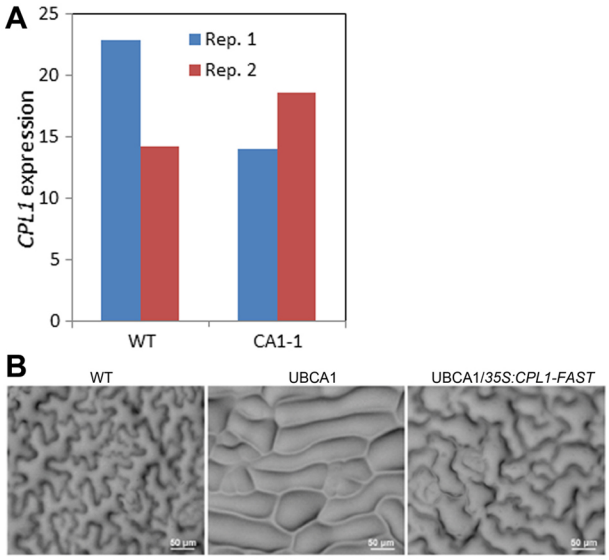

Fig. S8. Effect of *CA-rop2* expression in *CPL1* transcript level and suppression of CA-rop2 phenotype by *35S:CPL1-FAST*.
(*A*) *CA-rop2* expression does not affect *CPL1* transcription. The *CPL1* transcript level in WT (wild-type) and CA1-1 revealed by RNA Seq analysis was presented (total counts per million reads). Values for two biological replicates (Rep. 1 and Rep. 2) are presented. This is also consistent with regular RT-PCR result shown in Fig. 1D. (*B*) *35S:CPL1-FAST* suppressed the pavement cell shape phenotype of UBCA1. This suppression was similar to *35S:CPL1* (compared to Figure 3C). WT, wild-type.

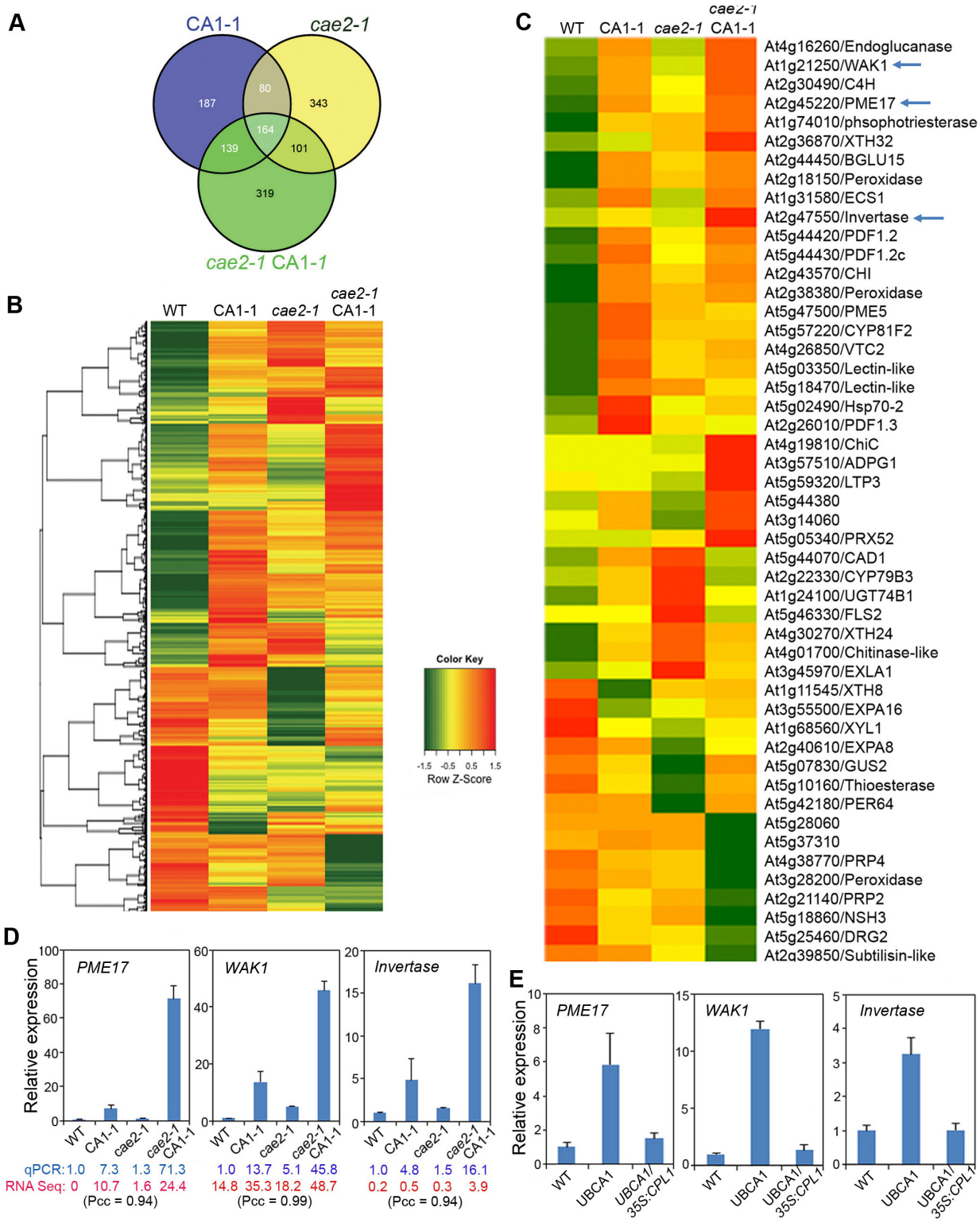

Fig. S9. Transcriptional regulation by CPL1 in ROP2 signaling.
(*A*) Heat map showing expression of 1,333 differentially regulated genes in CA1-1, *cae2-1* and *cae2-1* CA1-1, compared to WT (wild-type). (*B*) Venn diagram analysis of genes mis-regulated in CA1-1, *cae2-1* and *cae2-1* CA1-1. Mis-regulated genes were identified by comparing their

expression levels with the wild-type. (*C*) Heat map showing mis-regulation of 49 cell-walled related genes in CA1-1, *cae2-1* and *cae2-1* CA1-1. Arrows indicate the three genes that were verified for their expression using quantitative RT-PCR presented and altered by transgenic overexpression of *CPL1*. (*D*) Quantitative RT-PCR (qRT-PCR) analysis of *PME17*, *WAK1*, At2g47550/invertase genes in WT, CA1-1, *cae2-1*, *cae2-1* CA1-1 backgrounds. qPCR values are means ± SD (n=3). The qPCR and RNA sequencing (RNA Seq) results were listed below each genotype, with the values of corresponding Pearson correlation coefficient (Pcc) between these two measurements. (*E*) qRT-PCR analysis of *PME17*, *WAK1*, At2g47550/invertase genes in WT, UBCA1 and a *CPL1* overexpression line in the UBCA1 background (UBCA1/*35S:CPL1*). Values are means ± SD (n=3).

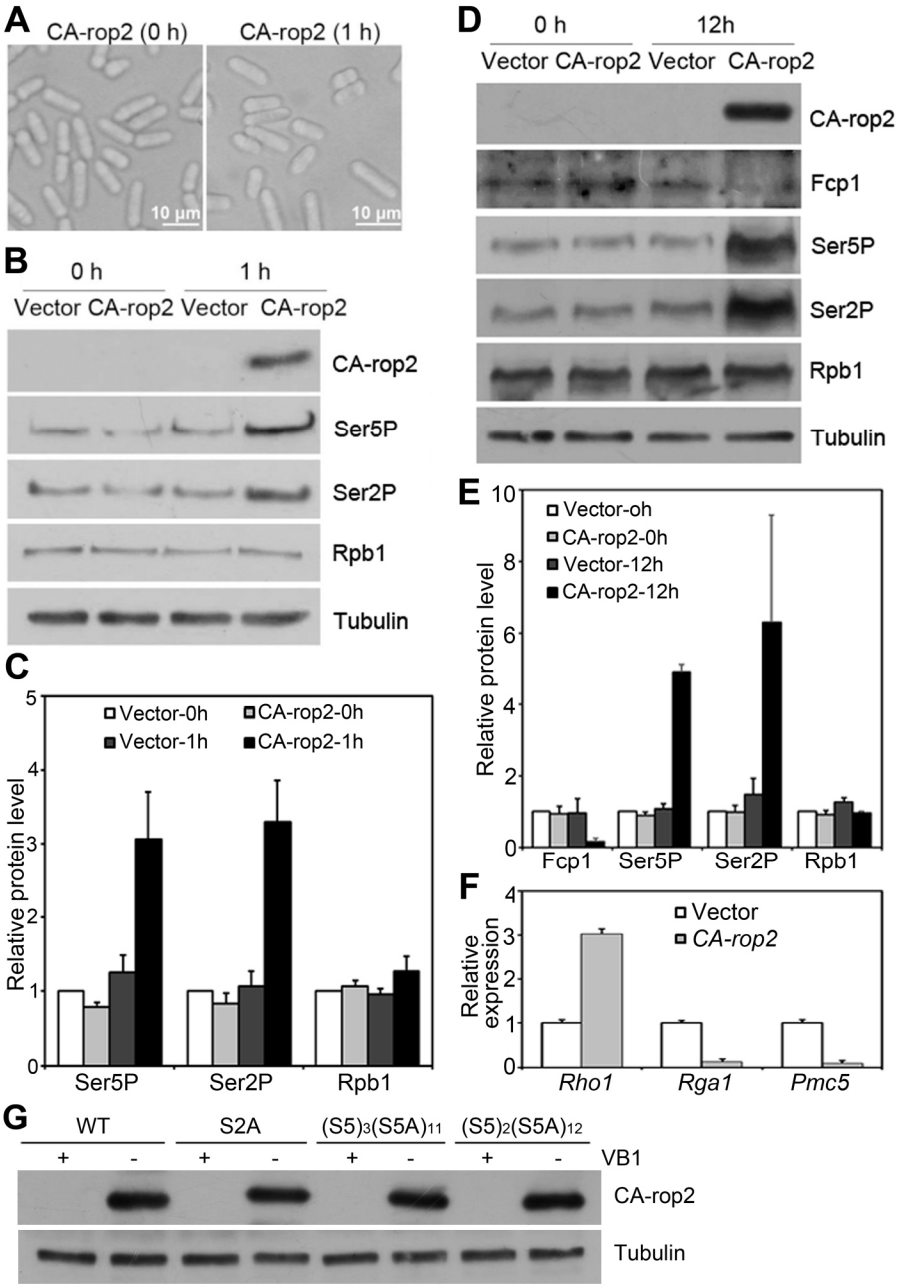

Fig. S10. Involvement of the Rho-CTD link in fission and budding yeast cells.
(*A* to *C*) Rapid stimulation of Ser5P and Ser2P by 1-hr induction of *CA-rop2* in fission yeast. (A) Yeast cell morphology after 1 hr of CA-rop2 induction. There was no difference between yeast strains transformed with vector and *CA-rop2* respectively. Vector, the empty vector control. (*B*) After 1-hr induction of *CA-rop2* expression, the level of Ser5P and Ser2P increased quickly without altering RPB1 protein level. Tubulin was used as a loading control. (*C*) Quantitative analysis of Ser5P and Ser2P after 1-hr induction of CA-rop2. (*D* and *E*) Fcp1 protein level decreased after 12 hrs of inducible expression of *CA-rop2* by galactose in budding yeast. An anti-Fcp1 antibody was used to detect Fcp1 level *in vivo*. Values in (*C* and *E*) are means ± SD

(n=3 biological replicates), with different letters indicating a statistical difference ($P<0.05$; Pair-wise *t*-test). (*F*) Altered expression of three cell shape-related genes by inducible expression of *CA-rop2* in fission yeast. Gene expression for the vector control was set to 1 after normalization using 18S rRNA as an internal standard. (G) Western blot showing similar induction of CA-rop2 protein expression in fission yeast wild-type (WT) and various S→A mutant strains. Proteins were extracted from cells grown in the presence of thiamine (+VB1; uninduced) or absence of thiamine (-VB1; induced) for 48 hrs. Tubulin was used as a loading control.

SI Table S1.

Primers used in this study.

Primer Name	Primer Sequences (5'→3')
CAM2	ATCGCAAGACCGGCAACAGGATTC
ZZP6	TA CTG CAG ACG GAT CAG GAT ATT CTT GT
ZZP7	CGAT CCATGG CGG TAG AGA GAA TTG AGA GA
ZZP10	GTA CCATGG GAG CTC GGT ACC CGG GGA TC
CZP17	TGT TCT ACA CGG AAT TGC TAT
CZP18	GCC TGA GAA CAA GCT AAA CG
CZP104	ACT GCC ACC ACA AAC GGT TGC
CZP181	TTA GAG ATG TGG AGG CTC CTT GAT CC
CZP192	GGAAGATCT TCATGTATAGTAATAATAGAGTAG
CZP193	AT CACGTG G TTAAGAGTATCTTCCCGAAGATG
CZP194	GGGGTACCCGTATATGAACAAGAGTCGGT
CZP195	TCGGTTGTTGAGGTTGTTGAAAT
CZP196	ATCACGTG GCAAGTTTCTCTGAGTCCGT
CZP201	AAA TAT AGA TCC GAG GAT AGC
CZP 261	GGA AGG AGT TGG ATC GAC AT
CZP262	TGT TTG ACA TCC CAC CAA AT
CZP278	GTT CTC TGT TGA GGC TTG GCT
BZP20	cgcg ctcgag ATGTATAGTAATAATAGAGTAG
BZP21	cg agatct TTAAGAGTATCTTCCCGAAG
BZP43	ctta ctcgag ATGGATACGAGGTTTCCGT
BZP44	GACACACGCTGTCATTTGAGA
BZP45	GATGATGCTGGAAGTAGTGCTC
BZP46	GGgGTaCCTGACACTGGTGAACGA
BZP78	AGCCACCAAAGCAGAAGAAG
BZP79	AAATGGGCCGAATCAAATAG
BZP81	cg ggatcc ATGGCGTCAAGGTTTATAAAG
BZP82	cg tctaga TCACAAGAACGCGCAACGGTTC
BZP100	ATTCTCCCCCAGAGGCTGAT
BZP101	TGCTTGATGCGACCTGATGT
BZP106	TAGGACCAAAGTGCCGTGAC

BZP107	TTTGCGCGTCGAGTTTTGAG
BZP118	cg ggatcc ATGGCGACGACAATGAAGGG
BZP119	acgc gtcgac TCAGATAATATCGTTACAGG
BZP132	CTagatct g AGAGTATCTTCCCGAAGATG
BZP133	gtg cta CTTCTCGAACTGTGGGTGAGA
BZP134	cgcg ctgcag ATGTATAGTAATAATAGAGTAG
BZP145	CGAAGATCCCTCTCACGAGC
BZP146	TGAACATCCTCGGCCCTAGA
BZP187	ATTCTGGTGTGTGCGCAATG
BZP193	AGGAACCTTTCCCGAGGTCT
BZP194	AGGGACGTAGACGGTCGTAA
BZP205	GGTTCAGTCGATGGGTGGTT
BZP206	ACCAGTCAGTCGCTTGAGTT
BZP213	ACCAACACCACCGAAACGAA
BZP214	ACGCTTTTCGAGACTCAGCA
28 S rRNA f	TGAGAAGGGATGTTGGACCTGCTT
28 S rRNA r	ATTGCGTCAACACCACTTTCTGGC